International Journal of Multiphase Flow 85 (2016) 278–283

Contents lists available at ScienceDirect

International Journal of Multiphase Flow

journal homepage: www.elsevier.com/locate/ijmultiphaseflow

Regimes of sediment-turbulence interaction and guidelines for simulating the multiphase bottom boundary layer

Justin R. Finn*, Ming Li

Centre for Engineering Sustainability, School of Engineering, University of Liverpool, Liverpool, UK

ARTICLE INFO

Article history:
Received 29 October 2015
Revised 8 April 2016
Accepted 9 June 2016
Available online 21 June 2016

Keywords:
Sediment transport
Particle turbulence interactions
Point particle approach
Fully resolved simulation

ABSTRACT

Characterizing the interaction of mobile sediments with a turbulent boundary layer driven by waves and currents represents an important scientific and engineering challenge. To approach this, Balachandar's scaling relations for particle Reynolds number and Stokes number (IJMF, vol. 35, pg 801–110, 2009) are recast in terms of Shields parameter and particle Galileo number. This allows for the modified Shields diagram to be partitioned into at least five regimes, where distinct primary mechanisms of sediment-turbulence interaction are identified. Practical guidelines are provided for selecting an appropriate direct or large-eddy simulation approach in the Shields-Galileo phase space.

1. Introduction

The transport of sediments in the bottom boundary layer due to forcing from currents, waves and tides can have lasting environmental, social and economic consequences (Mehta, 2014; van Rijn, 1993), which makes development of improved predictive capabilities for sediment motion a scientific and engineering priority. Since the majority of coastal, fluvial and estuarine sediment transport takes place under turbulent flow conditions, this objective cannot proceed without first understanding the nature of turbulent interactions with mobile sediments for a given field or laboratory condition.

When mobilized by a turbulent boundary layer flow, finite-size, heavier-than-fluid sediments will obtain a non-zero "slip velocity" due to both gravitational settling and interaction with turbulent eddies. This can lead to modulation of the turbulent kinetic energy spectrum via several coupled mechanisms (Balachandar and Eaton, 2010; Crowe, 2000; Yuan and Michaelides, 1992). For solid particles in a turbulent flow, vortex shedding and oscillation in the wake of particles has been proposed as the primary driver of turbulence enhancement (Hetsroni, 1989), and it has been argued that work done by the turbulent flow to continuously accelerate and decelerate heavy particles acts as a primary dissipative mechanism (Yuan and Michaelides, 1992). Theories developed from order of magnitude estimates and length and timescale arguments have generally confirmed this (Crowe, 2000; Kenning and Crowe, 1997; Yuan and Michaelides, 1992), and more recent experimental and numerical studies have further refined these ideas (Bagchi and Balachandar, 2004; Burton and Eaton, 2005; Ferrante and Elghobashi, 2003; Lucci et al., 2010; Tanaka and Eaton, 2010).

Using evidence from direct numerical simulation and experiments, Elghobashi (1991, 1994, 2006) developed a classification map of particle-turbulence interactions based on particle Stokes number, $St = \tau_p/\tau_k$ (ratio of particle to Kolmogorov timescale), and the solid volume fraction, ϕ, suggesting large St particles will enhance turbulence production, while small St particles will enhance dissipation. For flows with even modest concentrations, $10^{-6} < \phi < 10^{-3}$, particles can significantly modulate the turbulent energy spectrum (two-way coupling), and for denser suspensions, $\phi \gtrsim 10^{-3}$, particle-particle interactions (four-way coupling: e.g. collisions, drafting) further influence both the particle motion and turbulent spectra in complex ways. Building on these observations, Balachandar (2009) and Balachandar and Eaton (2010) developed explicit scaling relationships for the particle Reynolds number and Stokes number as a function of particle-to-fluid density ratio, and the ratio of particle size to Kolmogorov length scale. They then examined a hierarchy of available multiphase simulation approaches, namely the dusty-gas (DG), equilibrium Eulerian (EE), two-fluid (TF), point-particle (PP) and fully resolved simulation (FRS) methods[1]. They defined each method's range of applicability, as well as a "*method of choice*"- the approach which

* Corresponding author.
E-mail addresses: J.Finn@liv.ac.uk (J.R. Finn), M.Li@liv.ac.uk (M. Li).

[1] For a detailed discussion of these methods and their inherent limitations we refer the reader to Balachandar (2009); Balachandar and Eaton (2010).

http://dx.doi.org/10.1016/j.ijmultiphaseflow.2016.06.007

satisfies the restrictions of direct or large eddy simulation (DNS, LES) at the lowest perceived computational cost.

A wide range of St, and ϕ can be found in the bottom boundary layer, making effective parameterization of sediment-turbulence interactions a daunting task. In spite of this, incorporation of such effects into averaged equations models has generally helped to improve sediment transport predictions (see for example Amoudry et al., 2008; Hsu et al., 2004). At the same time, advances in both numerical modeling and computing capacity have begun to allow for fundamental DNS and LES studies of sediment-turbulence interactions in the multiphase wave and current bottom boundary layer using methods based on EE (Ozdemir et al., 2010; Penko et al., 2013), PP (Apte et al., 2008; Arolla and Desjardins, 2015; Finn et al., 2016; Schmeeckle, 2014), and FRS (Derksen, 2015; Ji et al., 2013; Kidanemariam and Uhlmann, 2014; Vowinckel et al., 2014), in conjunction with a model for four-way coupling interactions (collisions). While these approaches have produced extensive new insights, little practical guidance exists on their range of applicability for simulating the conditions of interest.

In this brief communication, we recast and further develop the scaling arguments of Elghobashi (1991) and Balachandar (2009) for the sediment transport problem so that the results can be examined in the framework of a modified Shields (1936) diagram, ie in terms of the Shields parameter, a non-dimensional shear stress,

$$\theta = \frac{u_\star^2}{(s-1)gd_p}, \tag{1}$$

and the Galileo number, a ratio of gravitational to viscous forces on a particle,

$$G = \frac{d_p\sqrt{(s-1)gd_p}}{\nu}. \tag{2}$$

Here, $u_\star$ is the friction velocity of the wave and/or current driven boundary layer, d_p is the particle diameter, $s = \rho_p/\rho_f$ is the particle-to-fluid density ratio, and g is the gravitational acceleration. This exercise allows us to (i) identify the dominant mechanism of sediment-turbulence interaction in terms of the non-dimensional groups important to sediment transport[2] (free surface effects and Froude number influence is neglected), and (ii) establish guidelines for simulating sediment-turbulence interactions in different regions of the G, θ, s phase space. Strictly speaking, the scaling developed by Balachandar (2009) is restricted to a dilute dispersed phase concentration. In the absence of a similar theory for densely laden conditions where four-way coupling is important (ie, bedload sediment transport), we believe this is still a useful starting point to examine the regimes of sediment-turbulence interaction.

2. Theory

For relatively dilute flow ($\phi \lesssim 0.001$), particle-turbulence interactions can be characterized using the particle Reynolds number, $Re_p = d_p|\boldsymbol{u}_p - \boldsymbol{u}_f|/\nu$, and the particle Stokes number, $St = \tau_p/\tau_k$. Even for dense flow conditions with four-way coupling, ie bedload dominated sediment transport, these parameters should remain important, in addition to ϕ. Here, ν is the kinematic viscosity of the fluid, $|\boldsymbol{u}_p - \boldsymbol{u}_f|$ is the slip velocity between the particle and the undisturbed ambient flow, τ_k is the Kolmogorov timescale, and the particle timescale, τ_p, is

$$\tau_p = \frac{2s+1}{36}\frac{d_p^2}{\nu}\frac{1}{f(Re_p)}, \tag{3}$$

where we assume the expression of Schiller and Naumann (1935) for the finite Reynolds number correction to the drag coefficient for spherical particles,

$$f(Re_p) = 1 + 0.15Re_p^{0.687}. \tag{4}$$

Reasonable alternatives to Eq. 4 exist that take into account the irregularity of natural sand grains (i.e. Fredsøe et al., 1992) and the influence of ϕ (Tenneti et al., 2011), but these effects are are not directly considered here.

If the Kolmogorov length scale in the boundary layer is estimated as $\eta = \nu/u_\star$, re-arrangement of Eqs. (1) and (2) provides the ratio of particle size to Kolmogorov length scale,

$$\frac{d_p}{\eta} = G\sqrt{\theta}. \tag{5}$$

Similarly, with $\tau_k = \eta^2/\nu$ and the definition of τ_p from Eq. (3), the Stokes number becomes,

$$St = \frac{\tau_p}{\tau_k} = \frac{2s+1}{36f(Re_p)}G^2\theta. \tag{6}$$

For $s > 1$, Re_p can be influenced by both turbulent eddies and gravitational settling. Balachandar (2009) described three regimes of particle timescale that govern the particle Reynolds number due to turbulence:

1. $\tau_p < \tau_k$: Both Re_p and St are less than one, and particle relative velocity is influenced primarily by the smallest scales of the turbulent flow.
2. $\tau_k < \tau_p < \tau_L$: The particle timescale is larger than the Kolmogorov scale but smaller than the integral scale of turbulence. Particle relative velocity is then influenced primarily by an intermediate scale eddy in the inertial range that has the same timescale as the particle. The size of this eddy is $l_i = \tau_p^{3/2}\epsilon^{1/2}$, where ϵ is the dissipation rate of the flow. Taking $\epsilon \approx \nu^3/\eta^4$ and using Eqs. (3) and (2), the ratio of particle size to l_i is,
$$\frac{d_p}{l_i} = \frac{216}{G^2\theta}\left(\frac{f(Re_p)}{2s+1}\right)^{3/2}. \tag{7}$$
3. $\tau_p > \tau_L$: The particle timescale is larger than the integral timescale of the flow, τ_L, and the particle relative velocity is limited by the integral velocity scale, u_L.

Ignoring the third regime, which is rare in the context of geophysical sediment transport, Balachandar's (2009) scaling for the turbulence related Reynolds number, $Re_{p,\,t}$, can be manipulated to provide one of two expressions depending on whether St is larger or smaller than unity,

$$Re_{p,t} = \begin{cases} \frac{s-1}{18f(Re_{p,t})}G^3\theta^{3/2} & \text{for} \quad G^2\theta \le \frac{36f(Re_p)}{2s+1} \\ \frac{s-1}{3\sqrt{(2s+1)f(Re_{p,t})}}G^2\theta & \text{for} \quad G^2\theta > \frac{36f(Re_p)}{2s+1} \end{cases}. \tag{8}$$

For heavier than fluid particles, gravitational settling will also induce a relative velocity, $w_s = \tau_p g\left(\frac{3}{2s+1}\right)$. Using Eq. (3), the settling related particle Reynolds number, $Re_{p,s} = w_s d_p/\nu$, becomes,

$$Re_{p,s} = \frac{G^2}{18f(Re_{p,s})}. \tag{9}$$

For the purposes of this note, we assume that the actual particle Reynolds number is due to either settling or turbulence, but not simultaneously both, and take Re_p to be the maximum of the turbulent and settling contributions,

$$Re_p = \max\left(Re_{p,t}, Re_{p,s}\right). \tag{10}$$

Finally, combining Eqs. (5) and (9) with the assumed relation for η, the suspension number (or scaled Rouse number),

[2] Our choice of parameters is not unique, and a number of similar re-scalings of Shields (1936) diagram can be found in the literature (Madsen and Grant, 1976; Van Rijn, 1984; Vanoni, 1975). The first appears to be the work of Bonnefille (1963).

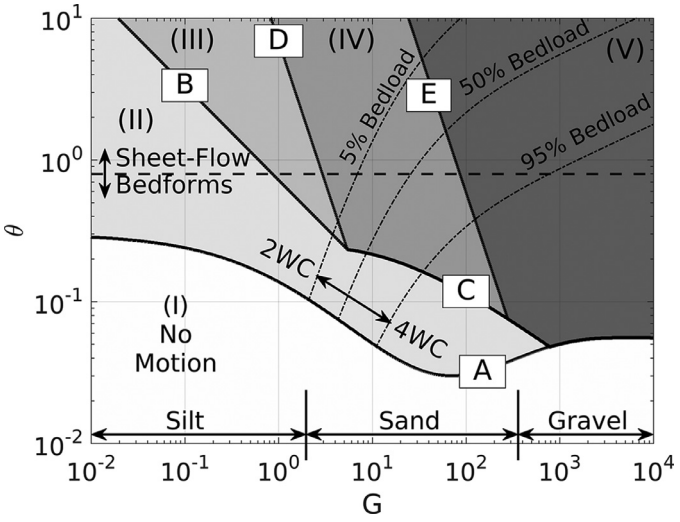

Fig. 1. Proposed regime map for sediment-turbulence interactions with $s = 2.65$ in the bottom boundary layer. Shading corresponds to regions having distinct primary particle slip-velocity mechanisms: Fixed bed (I), Gravitational settling (II), Kolmogorov interactions (III), Inertial range dissipation (IV), Inertial range production (V). Regime boundaries labeled A–E are given by Eqs. (12)–(16). The (- - -) line corresponds to the $\theta \approx 0.8$ transition between sheet-flow and bedform conditions. The (– · –) lines correspond to contours of constant bedload fraction observed experimentally by Roberts et al. (2003) for quartz sand in water: 95% bedload ($\mathcal{S} = 1.94$), 50% bedload ($\mathcal{S} = 0.77$), 5% bedload ($\mathcal{S} = 0.34$).

$\mathcal{S} = w_s/u_\star$, which characterizes the competition between particle settling and turbulent suspension, can be written

$$\mathcal{S} = \frac{Re_{p,s}}{G\sqrt{\theta}}. \tag{11}$$

Using kinematic arguments, Bagnold (1966) first developed a suspension criteria of the form, $\theta_{susp} \geq 0.4 w_s/gd_p$, corresponding to $\mathcal{S} = 1.23$.

3. Main result

For any θ, G and s all greater than 1, Eqs. (4), (6), (8), (9), and the assumption of Eq. (10) are uniquely determined and can be solved iteratively for St and Re_p. Here, we consider $10^{-2} \leq G \leq 10^4$ and $10^{-2} \leq \theta \leq 10^1$. Our discussion is framed around natural quartz sediments in water ($s = 2.65$, $g = 9.81\text{m/s}^2$, and $\nu = 10^{-6}\text{m}^2/\text{s}$), for which this parameter space corresponds to particle sizes ranging from fine silts ($d_p = 2\mu\text{m}$, neglecting cohesive effects) to gravels ($d_p = 2\text{cm}$), and Shields parameters between incipient motion and energetic sheet flows. For the interested reader, a small MATLAB® function that can evaluate similar results for any $s > 1$ is provided as supplementary material to this note.

The results for Re_p and St allow the Shields diagram to be partitioned into at least 5 regimes with distinct primary mechanisms of sediment-turbulence interaction, as shown in Fig. 1. The five regimes and their boundaries are defined as follows:

I **No motion**: For a given value of G, there is a critical value of Shields parameter, θ_{cr}, below which negligible particle motion occurs. Soulsby (1997) suggests one of many possible functional fits to experimental observations of θ_{cr}, which is plotted as line A in Fig. 1,

$$\theta_A = \theta_{cr} = \frac{0.3}{1 + 1.2G^{2/3}} + 0.055\left[1 - \exp\left(-0.02G^{2/3}\right)\right]. \tag{12}$$

Turbulent interactions with a fixed rough bed have a rich phenomenology of their own (van der A et al., 2011; Nielsen, 1992; Sleath, 1987), but we do not make further attempts to characterize them here.

II **Gravitational settling:** In this regime, which covers a wide range of particle sizes inclusive of silts, sands and gravels, gravitational settling is the main driver of relative velocity ($Re_{p,s} > Re_{p,t}$). Regime II is bound by Eq. (12) for small θ, and by $Re_{p,s} = Re_{p,t}$ for larger θ. Combining Eqs. (8) and (9), the latter condition results in two criteria, one for $St < 1$ and one for $St > 1$, shown as lines B & C in Fig. 1.

$$\theta_B = [G(s-1)]^{-2/3} \quad \text{for } G^2\theta \leq \frac{36}{2s+1} \tag{13}$$

$$\theta_C = \frac{\sqrt{2s+1}}{6(s-1)\sqrt{f(Re_p)}} \quad \text{for } G^2\theta > \frac{36}{2s+1} \tag{14}$$

For small G in regime II, to the left of the B-C-D intersection, $St < 1$, and line B corresponds to the transition described by Balachandar (2009) from $g/a_k > 1$ (settling dominates) to $g/a_k < 1$ (turbulence dominates), where $a_k = \nu^2/\eta^3$ is the acceleration associated with the Kolmogorov scale. For larger St, to the right of the B-C-D intersection, regime II particles may respond to the larger inertial scales of the flow, but their relative velocity will still primarily be dictated by gravitational settling. Note, we have used the fact that $Re_p|_{St=1} \lesssim 1$ to make approximation $f(Re_p|_{St=1}) \approx 1$, and write the $St = 1$ transition without dependence on $f(Re_p)$.

III **Kolmogorov interactions:** For a range of small particles with $St < 1$, at sufficiently high θ the relative velocity due to the interactions with the Kolmogorov scales will exceed the gravitational settling velocity and the particles will behave almost as tracers for the smallest scales of fluid motion. For $s = 2.65$, regime III covers mostly sheet flow conditions for silt and fine sands. The upper limit on θ for this regime, shown as line D, is given explicitly by setting $St = 1$ in Eq. (6) and again assuming $f(Re_p|_{St=1}) \approx 1$,

$$\theta_D = \frac{36}{(2s+1)G^2}. \tag{15}$$

IV **Inertial range dissipation:** Two regimes can be identified where $St > 1$ and the particle relative velocity will be dictated primarily by an inertial eddy scale, l_i, as defined in Eq. (7). In regime IV, which corresponds to mostly sand-size particles over a wide range of θ for $s = 2.65$, these interactions are expected to have a net dissipative effect on the turbulence so long as the particle Reynolds number does not exceed some transitional threshold value, Re_{tr}.

V **Inertial range production:** In this regime, $Re_p > Re_{tr}$, and the presence of the particles should result in a net production of turbulence. This is due to the augmentation of turbulence by oscillating particle wakes and introduction of particle scale turbulence through vortex shedding, which may start at a somewhat smaller value of Re_p, but becomes dominant relative to particle induced dissipation at higher Re_p. The threshold at which this occurs, and thus the transition from regime IV to regime V (line E), is determined by setting $Re_p = Re_{tr}$ in Eq. (8),

$$\theta_E = \frac{3Re_{tr}\sqrt{(2s+1)f(Re_{tr})}}{(s-1)G^2}, \tag{16}$$

Evidence suggests that $Re_{tr} \approx 400$ (Elghobashi, 1991; Hetsroni, 1989), and this has been used to plot line E in Fig. 1. It is interesting to note that continuation of line E down to line A produces a small additional regime for $s = 2.65$ (not explicitly marked), where gravitational settling of large particles may further enhance production of turbulence ($Re_{p,s} > Re_{tr}$). This additional regime vanishes for heavier sediments ($s \gtrsim 5$) but becomes larger for lightweight sediments ($1 < s < 2.5$), which are more easily suspended at low θ. It could be relevant to

the "lower plane bed" regime found for coarse sand and gravel transport (Simons and Richardson, 1961).

Also shown in Fig. 1 as the $(- - -)$ line is the approximate transition from bedform (dunes, ripples) conditions to more energetic sheet flow conditions at $\theta \approx 0.8$. Bedforms can strongly influence bottom boundary layer hydrodynamics by introducing large scale coherence, rhythmic vortex shedding, and an enhanced effective roughness (Nielsen, 1992), which may have implications for the region boundaries described above. Perhaps more important are the transitions marked by $(- \cdot -)$ lines, which correspond to constant suspension number, $\mathcal{S}$. Recent tilting flume measurements by Roberts et al. (2003) have suggested that the proportion of sediment carried as bedload is roughly constant for constant $\mathcal{S}$. The $(- \cdot -)$ lines shown in Fig. 1 correspond to their results for 5% bedload ($\mathcal{S} = 0.34$), 50% bedload ($\mathcal{S} = 0.77$), and 95% bedload ($\mathcal{S} = 1.94$) for quartz sediments in water. For conditions where most of the sediment is carried as suspended load (low $\mathcal{S}$), the dominant sediment-turbulence interactions will result from two-way coupling (2WC) and the scaling arguments developed here should be sound. As the fraction of sediment transported as bedload is increased (large $\mathcal{S}$), particle-particle interactions and four way coupling (4WC) in the high concentration layer near the bed will play an increasingly important role in overall turbulence modulation. Effective parameterization of 4WC effects is an important and ongoing effort, and the arguments used to construct Fig. 1 can and should be updated as the effects of strong 4WC in the bottom boundary layer become better understood.

4. Implications for direct and large eddy simulation

By transforming the Re_p and St scaling into the $G - \theta$ space, some comments can be made regarding the range of applicability of available DNS and LES modeling approaches.

When performing DNS, regardless of the approach adopted to handle the particle phase, all scales of fluid motion from η to L, including those introduced by the particles, should be resolved by the grid spacing. Strictly speaking, this limits the applicability of EE, TF, and PP approaches to conditions where $d_p < l_k$. The continuum based EE and TF approaches should also respect the Stokes number restrictions $St_{EE} \lesssim 0.2$ and $St_{TF} \lesssim 1$ (Balachandar, 2009; Ferry and Balachandar, 2001). Using Eqs. (5) and (6), these restrictions become,

$$\theta_{EE}^{DNS} < \max\left(\frac{1}{G^2}, \frac{7.2}{(2s+1)G^2}\right) \tag{17}$$

$$\theta_{TF}^{DNS} < \max\left(\frac{1}{G^2}, \frac{36}{(2s+1)G^2}\right) \tag{18}$$

$$\theta_{PP}^{DNS} < \frac{1}{G^2} \tag{19}$$

With this in mind, the modified Shields diagram for $s = 2.65$ is partitioned based on the method of choice for DNS in Fig. 2a. Only a modest region of the $G - \theta$ plane, corresponding to fine sands and silts in regimes II & III that satisfy $d_p/\eta < 1$ ($\theta < 1/G^2$), does not require a FRS approach to satisfy the DNS restrictions. Here, the less expensive EE approach becomes the method of choice because $St < 0.2$ is also satisfied for $s = 2.65$. There is no region of the $G - \theta$ phase space where either the TF or PP approach become the method of choice for DNS at this density ratio. For reference, previous EE-DNS and FRS simulations by several groups at $s \approx 2.65$ are also shown.

For LES, the grid size/particle size requirement can be relaxed to $\tau_p > \tau_\Delta$, where Δ is the LES filter size, and τ_Δ is the timescale of the smallest eddy resolved by this filter. This requirement ensures

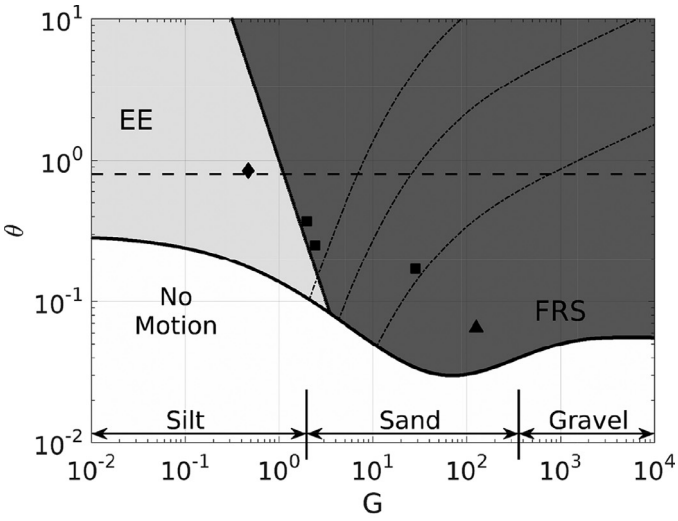

(a) DNS

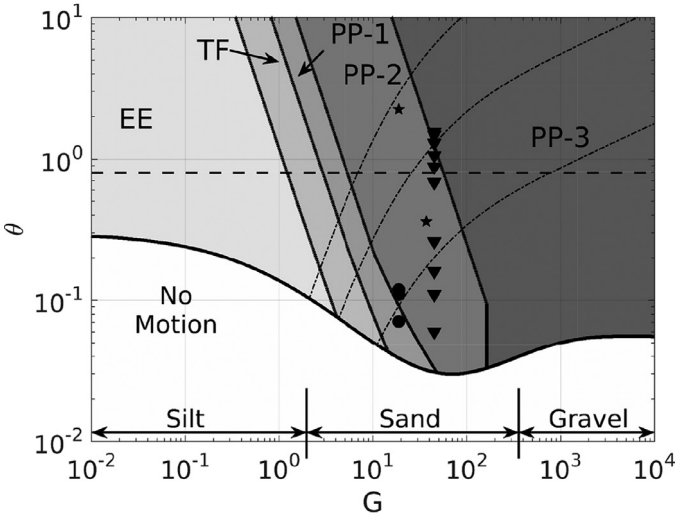

(b) LES

Fig. 2. Method of choice for direct and large eddy simulation of wave & current boundary layers at $s = 2.65$. Shown for reference are the EE-DNS simulations of Ozdemir et al. (2010)(✦), FRS simulations of Kidanemariam and Uhlmann (2014) (■), Ji et al. (2013)(▲), and the PP-LES simulations of Finn et al. (2016) (⋆), Schmeeckle (2014) (▼), and Arolla and Desjardins (2015) (●). The (- - -) and $(- \cdot -)$ lines are same as in Fig. 1.

that the dominant scale of particle-fluid relative velocity (due to the l_i scale eddies) is resolved. Setting $\Delta = l_i$, and using Eq. (5), a requirement for the ratio Δ/η can be derived,

$$\frac{\Delta}{\eta} \leq \frac{G^3\theta^{3/2}}{216}\left[\frac{2s+1}{f(Re_p)}\right]^{3/2}. \tag{20}$$

The method of choice for LES is shown in Fig. 2b. The region of EE applicability is roughly the same as for DNS, and there is a modest size region covering fine sands where $0.2 < St < 1$ is satisfied and the TF approach may become an optimal choice. At first glance, relaxing the particle size requirement does allow for the PP-LES approach to cover the remainder of the Shields diagram, however, two practical limitations must still be considered. First, it is not practical to push the PP-LES method to use LES filter widths much smaller than $\Delta \approx d_p$. Comparing Eq. (20) to the ratio d_p/η (Eq. (5)), it is clear that the required filter size is larger than d_p only

when,

$$\theta_{PP}^{LES} > \frac{216}{G^2}\left(\frac{f(Re_p)}{2s+1}\right)^{3/2}. \quad (21)$$

Second, sub-particle-scale wake interactions can contribute significantly to particle motion and turbulence modulation at higher Re_p (Bagchi and Balachandar, 2003; 2004; Burton and Eaton, 2005), and these effects are not naturally handled with standard point-particle LES closures. It is anticipated that both FRS and sub-particle-scale measurements (i.e. Tanaka and Eaton, 2010) can aid in the development of such models in the near future (Prosperetti, 2015). For the time being, assuming these effects become important when vortex shedding sets in, around a critical particle Reynolds number of $Re_{cr} \approx 210$ (Bagchi and Balachandar, 2004), then Eqs. (8) and (9) provide one of two restrictions, depending on whether $Re_{p,t}$ or $Re_{p,s}$ is larger,

$$\theta_{PP}^{LES} \lesssim \frac{3Re_{cr}\sqrt{(2s+1)f(Re_{cr})}}{(s-1)G^2} \quad (Re_{p,t} > Re_{p,s}) \quad (22)$$

$$G_{PP}^{LES} \lesssim \sqrt{18Re_{cr}f(Re_{cr})} \quad (Re_{p,t} < Re_{p,s})$$

The $G-\theta$ space for $St > 1$ can then be divided into three regions where PP-LES is either *the method of choice* or may be *the only viable choice*, assuming FRS is not computationally feasible:

1. **PP-1**: This regime corresponds to particles with $St > 1$ and where Eq. (21) is not easily satisfied, meaning Δ should be less than d_p to resolve the l_i scale and its interaction with the d_p size particles. Neither the TF-LES approach or the PP-LES approach are well suited to perform simulations here, without additional stochastic models to account for the sub-grid-scale contributions to the slip velocity (i.e. Pozorski and Apte, 2009). This is an important region of the Shields diagram, as it covers fine and medium sands commonly found on beaches and in estuaries.
2. **PP-2**: The inequalities of Eqs. (21) and (22) are satisfied, meaning that the particle's slip velocity can be predicted from the resolved fluid motions, and the particles are not expected to introduce significant sub-particle scale turbulence. To date, the PP-LES simulations reported in the literature for $s \approx 2.65$ (Arolla and Desjardins, 2015; Finn et al., 2016; Schmeeckle, 2014) almost all fall into this region.
3. **PP-3**: Here, Re_p is large enough that Eq. (22) cannot be satisfied meaning additional models need to be introduced to account for the sub-particle scale turbulence introduced by the sediment. Throughout this regime $d_p/\eta >> 1$ for $s = 2.65$. In this case, a numerically challenging, but perhaps more appropriate strategy would be to combine an interface resolving method with LES (for example, Ramakrishnan et al., 2009), thereby resolving the inertial range scales introduced by the sediment, but modeling the dissipative scales much smaller than d_p.

5. Concluding remarks

In this short communication Balachandar's scaling for particle Reynolds and Stokes number have been recast into the non-dimensional groups G, θ, and s, allowing the modified Shields diagram to be partitioned into (at least) 5 regimes with unique primary sediment-turbulence interaction mechanisms for a given value of s. Guidelines and practical restrictions have also been provided to the reader for selecting an appropriate numerical modeling approach for DNS or LES of the wave/current boundary layer in terms of these variables. The transitions between regimes shown in Figs. 1 and 2 are expected to be reasonable approximations, where before no such guidance was available. However, they should not be taken as sharp and inflexible; The physical mechanisms involved in sediment turbulence interaction in natural environments are indeed complicated and the results here can be updated as new understanding is developed. As is apparent from the results presented, in order to simulate many important regimes of the $G-\theta$ phase space, established modeling approaches need to be pushed, perhaps beyond their strict limitations, and new approaches should be explored.

Acknowledgments

This research received support from the UK Engineering and Physical Science Research Council (EPSRC) through the UK/Dutch SINBAD project (EP/J005541/1). We thank the anonymous referees, Professor S. Balachandar, and Joep van der Zanden for constructive feedback, which led to many improvements in the work.

Supplementary material

Supplementary material associated with this article can be found, in the online version, at 10.1016/j.ijmultiphaseflow.2016.06.007

References

Amoudry, L., Hsu, T.-J., Liu, P.-F., 2008. Two-phase model for sand transport in sheet flow regime. J. Geophys. Res. Oceans (1978–2012) 113 (C3), C03011–C03025.
Apte, S., Mahesh, K., Lundgren, T., 2008. Accounting for finite-size effects in simulations of disperse particle-laden flows. Int. J. Multiph. Flow 34 (3), 260–271.
Arolla, S.K., Desjardins, O., 2015. Transport modeling of sedimenting particles in a turbulent pipe flow using euler-lagrange large eddy simulation. Int. J. Multiph. Flow 75, 1–11.
Bagchi, P., Balachandar, S., 2003. Effect of turbulence on the drag and lift of a particle. Phys. Fluids (1994-present) 15 (11), 3496–3513.
Bagchi, P., Balachandar, S., 2004. Response of the wake of an isolated particle to an isotropic turbulent flow. J. Fluid Mech. 518, 95–123.
Bagnold, R.A., 1966. An Approach to the Sediment Transport Problem from General physics. Geological Survey Professional Paper 422-I. Government Printing Office, United States, pp. 231–291.
Balachandar, S., 2009. A scaling analysis for point–particle approaches to turbulent multiphase flows. Int. J. Multiph. Flow 35 (9), 801–810.
Balachandar, S., Eaton, J.K., 2010. Turbulent dispersed multiphase flow. Ann. Rev. Fluid Mech. 42, 111–133.
Bonnefille, R., 1963. Essais de synthèse des lois de début dentraînement des sédiments sous laction dun courant en régime continu. Bulletin Centre de Recherhce Chatou 5, 67–72.
Burton, T.M., Eaton, J.K., 2005. Fully resolved simulations of particle-turbulence interaction. J. Fluid Mech. 545, 67–111.
Crowe, C.T., 2000. On models for turbulence modulation in fluid–particle flows. Int. J. Multiph. Flow 26 (5), 719–727.
Derksen, J.J., 2015. Simulations of granular bed erosion due to a mildly turbulent shear flow. J. Hydraul. Res. 53 (5), 622–632.
Elghobashi, S., 1991. Particle-laden turbulent flows: direct simulation and closure models. Appl. Sci. Res. 48 (3–4), 301–314.
Elghobashi, S., 1994. On predicting particle-laden turbulent flows. Appl. Sci. Res. 52 (4), 309–329.
Elghobashi, S., 2006. An updated classification map of particle-laden turbulent flows. In: IUTAM Symposium on Computational Approaches to Multiphase Flow. Springer, pp. 3–10.
Ferrante, A., Elghobashi, S., 2003. On the physical mechanisms of two-way coupling in particle-laden isotropic turbulence. Phys. Fluids (1994-present) 15 (2), 315–329.
Ferry, J., Balachandar, S., 2001. A fast eulerian method for disperse two-phase flow. Int. J. Multiph. Flow 27 (7), 1199–1226.
Finn, J.R., Li, M., Apte, S.V., 2016. Particle based modeling and simulation of natural sand dynamics in the wave bottom boundary layer. J. Fluid Mech 796, 340–385.
Fredsøe, J., Deigaard, R., et al., 1992. Mechanics of Coastal Sediment Transport, vol.3. World Scientific.
Hetsroni, G., 1989. Particles-turbulence interaction. Int. J. Multiph. Flow 15 (5), 735–746.
Hsu, T.-J., Jenkins, J.T., Liu, P.L.-F., 2004. On two-phase sediment transport: sheet flow of massive particles. R. Soc. Lond. Proc. Ser. A 460, 2223–2250.
Ji, C., Munjiza, A., Avital, E., Ma, J., Williams, J., 2013. Direct numerical simulation of sediment entrainment in turbulent channel flow. Phys. Fluids (1994-present) 25 (5), 056601.
Kenning, V., Crowe, C., 1997. On the effect of particles on carrier phase turbulence in gas-particle flows. Int. J. Multiph. Flow 23 (2), 403–408.
Kidanemariam, A.G., Uhlmann, M., 2014. Direct numerical simulation of pattern formation in subaqueous sediment. J. Fluid Mech. 750, R2.
Lucci, F., Ferrante, A., Elghobashi, S., 2010. Modulation of isotropic turbulence by particles of taylor length-scale size. J. Fluid Mech. 650, 5–55.

Madsen, O.S., Grant, W.D., 1976. Quantitative description of sediment transport by waves. In: Proceedings of the Coastal Engineering, 1 (15).
Mehta, A.J., 2014. An Introduction to the Hydraulics of Fine Sediment Transport. World Scientific.
Nielsen, P., 1992. Coastal Bottom Boundary Layers and Sediment Transport, vol.4. World scientific.
Ozdemir, C.E., Hsu, T.-J., Balachandar, S., 2010. A numerical investigation of fine particle laden flow in an oscillatory channel: the role of particle-induced density stratification. J. Fluid Mech. 665, 1–45.
Penko, A., Calantoni, J., Rodriguez-Abudo, S., Foster, D., Slinn, D., 2013. Three-dimensional mixture simulations of flow over dynamic rippled beds. J. Geophys. Res. Oceans 118 (3), 1543–1555.
Pozorski, J., Apte, S.V., 2009. Filtered particle tracking in isotropic turbulence and stochastic modeling of subgrid-scale dispersion. Int. J. Multiph. Flow 35 (2), 118–128.
Prosperetti, A., 2015. Life and death by boundary conditions. J. Fluid Mech. 768, 1–4.
Ramakrishnan, S., Zheng, L., Mittal, R., Najjar, F., Lauder, G., Hedrick, T., 2009. Large eddy simulation of flows with complex moving boundaries: application to flying and swimming in animals. In: Proceedings of the 39th AIAA Fluid Dynamics Conference, AIAA, vol. 3976. San Antonio, TX.
Roberts, J.D., Jepsen, R.A., James, S.C., 2003. Measurements of sediment erosion and transport with the adjustable shear stress erosion and transport flume. J. Hydraul. Eng. 129 (11), 862–871.
Schiller, L., Naumann, Z., 1935. A drag coefficient correlation. Ver. Deutsch. Ing. 77 (318), 51.
Schmeeckle, M.W., 2014. Numerical simulation of turbulence and sediment transport of medium sand. J. Geophys. Res. Earth Surf. 119 (6), 1240–1262.
Shields, A., 1936. Application of Similarity Principles and Turbulence Research to Bed-Load Movement. Technical Report. Soil Conservation Service.
Simons, D.B., Richardson, E.V., 1961. Forms of bed roughness in alluvial channel. J. Hydraul. Div. 87 (3), 87–105.
Sleath, J., 1987. Turbulent oscillatory flow over rough beds. J. Fluid Mech. 182, 369–409.
Soulsby, R., 1997. Dynamics of marine Sands: A Manual for Practical Applications. Thomas Telford.
Tanaka, T., Eaton, J.K., 2010. Sub-Kolmogorov resolution partical image velocimetry measurements of particle-laden forced turbulence. J.Fluid Mech. 643, 177–206.
Tenneti, S., Garg, R., Subramaniam, S., 2011. Drag law for monodisperse gas–solid systems using particle-resolved direct numerical simulation of flow past fixed assemblies of spheres. Int. J. Multiph. Flow 37 (9), 1072–1092.
van der A, D.A., ODonoghue, T., Davies, A.G., Ribberink, J.S., 2011. Experimental study of the turbulent boundary layer in acceleration-skewed oscillatory flow. J. Fluid Mech. 684, 251–283.
Van Rijn, L.C., 1984. Sediment transport, part i: bed load transport. J. Hydraul. Eng. 110 (10), 1431–1456.
van Rijn, L.C., 1993. Principles of Sediment Transport in Rivers, Estuaries and Coastal Seas, vol. 1006. Aqua publications Amsterdam.
Vanoni, V., 1975. Sedimentation Engineering. ASCE. manuals and reports on engineering practice (54)
Vowinckel, B., Kempe, T., Fröhlich, J., 2014. Fluid–particle interaction in turbulent open channel flow with fully-resolved mobile beds. Adv. Water Resour. 72, 32–44.
Yuan, Z., Michaelides, E., 1992. Turbulence modulation in particulate flows - A theoretical approach. Int. J. Multiph. Flow 18 (5), 779–785.